

# Synthesis and characterization of some Schiff bases derived from orthophthalaldehyde and their bridged complexes with Co (II) and Ni (II) as corrosion inhibitors for carbon steel in acidic medium

Atheer Naji Abulhail\*, Mouayed Yousif Kadhum\*

Department of Chemistry, College of Education for Pure Sciences, University of Basrah, Basrah, Iraq

## ARTICLE INFO

Received 10 April 2024  
Accepted 30 May 2024  
Published 30 June 2024

## Keywords :

Schiff base, ortho-phthalaldehyde, inhibitors, corrosion

## ABSTRACT

In this study, two Schiff base ligands, L<sub>1</sub> and L<sub>2</sub> derived from ortho-phthalaldehyde and primary amines (4-aminopyridine and 4-aminobenzothiazole) were studied using infrared spectroscopy (IR), proton nuclear magnetic resonance spectroscopy (<sup>1</sup>HNMR), carbon-13 atomic magnetic coupled resonance spectroscopy (<sup>13</sup>CNMR), mass spectrometry, and also were performed by elemental analysis, and then reacted with tetrathiocyanates in a 1:1 molar ratio with Schiff base ligands synthesized to produce diatomic mixed-metal-bridge complexes as (L<sub>1</sub>MCd(SCN)<sub>4</sub>), where M represents Co(II) or Ni(II). These complexes were characterized by spectroscopic methods and magnetic susceptibility measurements. The results showed that all the complexes had the same coordination number of four. In addition, the cobalt complex exhibited paramagnetic properties, while the nickel complex exhibited diamagnetic properties. The synthesized Schiff base ligands were evaluated as an inhibitor of carbon steel corrosion in acidic medium and showed good inhibitory activity.

**Citation:** Atheer N. A., Mouayed Y. K., J. Basrah Res. (Sci.) 50(1), 251 (2024).  
DOI: <https://doi.org/10.56714/bjrs.50.1.20>

## 1. Introduction

It was first synthesized by scientist Hugo Schiff in 1864 [1] by direct addition of a primary amine carbonyl (aldehyde or ketone), and Schiff's principles are used to describe physical properties such as [2] there are double bonds between carbon and nitrogen atoms in structure). in various fields of science and engineering the Schiff basis is important [3]. They play important roles in important biological processes, such as non-enzymatic transamination reactions, and some reactions catalyzed by vitamin B6 [4] and certain Schiff bases have been shown to have anticancer effects [5]. They also exhibit antibacterial and antifungal properties, act as anti-inflammatory and analgesic agents, and are used as plant growth promoters Schiff uses pigment dyes with high

\*Corresponding author email : [atheer.naji@uobasrah.edu.iq](mailto:atheer.naji@uobasrah.edu.iq)



concentrations of metal ions due to the fact that they are composed of polydentate ligands. Due to their reaction-ability, the formation of valuable metal complexes is simple. Calculation methods [6]. Technological Importance The epoxidation of olefins in Schiff base has wide application and is used as antioxidants and catalysts. They also act as degraders and stabilizers in polymers, fuels, and as promoters of polymerization processes [7]. Also, Schiff bases are used as corrosion inhibitors, effectively inhibiting the corrosion of carbon steel [8-10], copper [11,12], aluminum [13,14], and other metals.

## 2. Materials and Instruments

The following reagents were used in this experiment: orthophthalaldehyde (obtained from TCI), 4-aminopyridine, and 4-aminobenzothiazole (obtained from Sigma Aldrich). All chemicals used were also obtained from Sigma Aldrich. These chemicals purity is 99%. A carbon steel alloy N80 with dimensions of 3 cm x 2 cm x 0.2 cm (length x width x thickness) was used in the experiment. FT-IR spectra were recorded on a Shimadzu FT-IR 8400S spectrophotometer equipped with a KBr sphere in the range of 4000-400  $\text{cm}^{-1}$  on a Bruker 500 NMR in the Department of Chemistry, analyzer Tehran University of Science and Technology Central Laboratory of Science and Technology, Islamic Republic of Iran.  $^1\text{H}$  NMR and  $^{13}\text{C}$  NMR spectra using spectrophotometer. Chemical compositions were measured using an Agilent Technologies 5975C mass spectrometer (EI) in Tarbiat Modares University, Tehran, 1999 laboratories, Iran.

## 3. Synthesis of Compounds

### 3.1. Synthesis of Schiff Base Ligands Text

In a 100 ml round bottom flask, fitted with a condenser and stopper, 10 mmol of aldehyde was added and then 20 ml of absolute ethanol and two drops of glacial acetic acid were added as catalysts. Gradually, 20 mmol of amine dissolved in 20 ml absolute ethanol was added to the mixture with constant stirring (Fig. 1). The mixture was refluxed when indicated. The mixture was subsequently cooled to room temperature. A portion of the solvent evaporated at reduced pressure, producing precipitates. The precipitate was filtered, washed, and recrystallized with appropriate treatment [15]. Table (1) shows the basic physical properties of Schiff bases and the optimum conditions for their fabrication.

**Table 1.** Some physical properties of Schiff bases and the optimal conditions for their synthesis

Sym.	Type of aldehyde	Type of amine	Time of reaction (hrs)	Recrystalline Solvent	colour and Physical state	Melting Point ( $^{\circ}\text{C}$ )	Yield%
L <sub>1</sub>	Ortho Phthalaldehyde 1.34 g	4-Aminopyridine 1.88 g	5	Ethanol	Yellow powder	250-252	88
L <sub>2</sub>	Ortho Phthalaldehyde 1.34 g	2-Amino benzothiazole 3 g	8	Ethanol	Brown powder	247-249	62

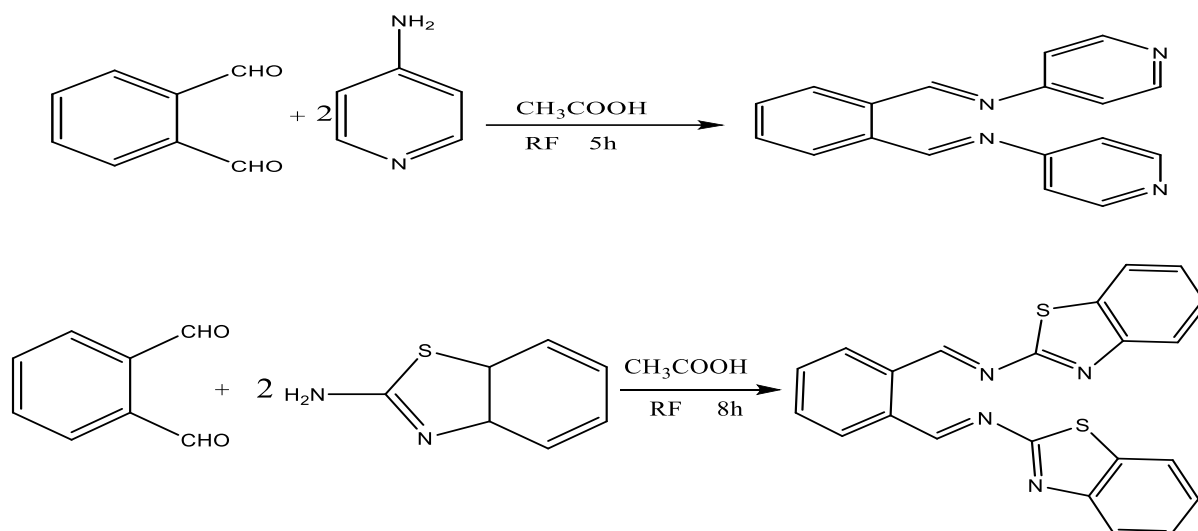


**Fig. 1.** Synthesis of ligands  $L_1$  and  $L_2$

### 3.2. Synthesis of Thiocyanate Complexes

Metal dithiocyanate [ $\text{Co}(\text{SCN})_2$ ,  $\text{Ni}(\text{SCN})_2$ ,  $\text{Cd}(\text{SCN})_2$ ] was synthesized by the reaction of metal nitrate with potassium thiocyanate in methanol. The potassium nitrate formed was removed by filtration, and the dithiocyanate product was retained for further reactions. For the preparation of  $\text{MCd}(\text{SCN})_4$  solution, where  $M = \text{Co}$ ,  $\text{Ni}$ ,  $\text{M}(\text{SCN})_2$  and  $\text{Cd}(\text{SCN})_2$  solutions were mixed in 1:1 molar ratio and stirred for 24 hours and then dry the resulting product and tetrathiocyanate were mixed with Schiff base synthesized in the same solvent at a molar ratio of 1:1 and stirred for 36 h. In each case, a solid was formed, filtered and extracted with methanol and water wash it [16]. The proposed solid structure is given in Fig. 2, and the necessary physical properties and optimal conditions are shown in Table 2.

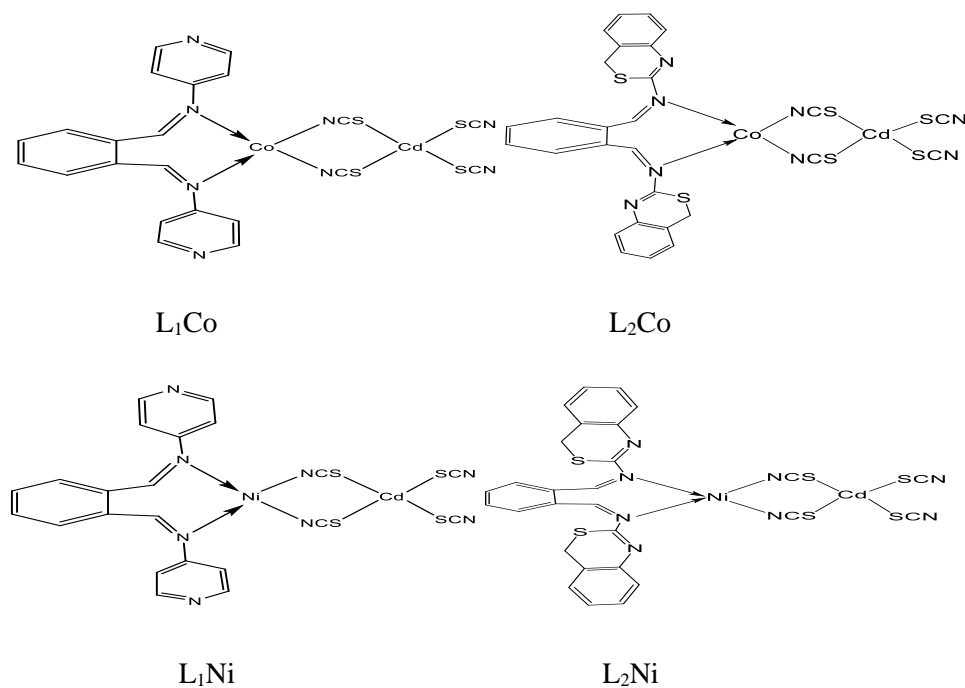


**Fig. 2.** Proposed structure of the prepared complexes

**Table 2.** Some physical properties and optimal conditions for their preparation

Sym.Of Complex	MCd(SCN) <sub>4</sub> (g) Ligand (g)	Molecular formula	colour and Physical state	Melting Point (°C)	Yield %
L <sub>1</sub> Co	0.4036 g L <sub>1</sub> (0.2861 g)	CoCd (SCN) <sub>4</sub> . C <sub>18</sub> H <sub>14</sub> N <sub>4</sub>	Olive powder	>250	78
L <sub>2</sub> Co	0.4036 g L <sub>2</sub> (0.3985 g)	CoCd (SCN) <sub>4</sub> C <sub>22</sub> H <sub>14</sub> N <sub>4</sub> S <sub>2</sub>	dark green powder	>250	80
L <sub>1</sub> Ni	0.4034 g L <sub>1</sub> (0.2861 g)	NiCd (SCN) <sub>4</sub> . C <sub>18</sub> H <sub>14</sub> N <sub>4</sub>	Green powder	>250	66
L <sub>2</sub> Ni	0.4034 g L <sub>2</sub> (0.3985 g)	NiCd (SCN) <sub>4</sub> C <sub>22</sub> H <sub>14</sub> N <sub>4</sub> S <sub>2</sub>	Light green powder	>250	62

## 4. Results and Discussion

### 4.1. Elemental analysis

The percentages of carbon, hydrogen, and nitrogen in the Schiff base ligand and its prepared complexes were estimated using a precision elemental analysis instrument. The results showed a correspondence between the practical percentages of the elements (carbon, hydrogen, nitrogen) and the theoretical calculated percentages. This confirms the validity of the proposed chemical structures for these prepared compounds [16], as illustrated in Table 3.

**Table 3 .** Elemental analysis data of the ligand and its complexes

Symb.of comp.	Molecular weight gm/mole	C%		H%		N%	
		Found	Cal.	Found	Cal.	Found	Cal.
L <sub>1</sub>	286 C <sub>18</sub> H <sub>14</sub> N <sub>4</sub>	75.50	74.23	4.93	5.05	19.57	18.99
L <sub>2</sub>	298 C <sub>22</sub> H <sub>14</sub> N <sub>4</sub> S <sub>2</sub>	66.31	64.96	3.54	2.99	14.06	14.73
L <sub>1</sub> Co	690 C <sub>18</sub> H <sub>14</sub> N <sub>4</sub> CoCd (SCN) <sub>4</sub>	38.3	38.84	2.05	1.94	16.24	15.96
L <sub>2</sub> Co	830 C <sub>22</sub> H <sub>14</sub> N <sub>4</sub> S <sub>2</sub> CoCd (SCN) <sub>4</sub>	40.51	41.02	2.19	1.98	13.5	14.06
L <sub>1</sub> Ni	690 C <sub>18</sub> H <sub>14</sub> N <sub>4</sub> NiCd (SCN) <sub>4</sub>	38.31	39.03	2.05	2.33	16.25	15.83
L <sub>2</sub> Ni	830 C <sub>22</sub> H <sub>14</sub> N <sub>4</sub> S <sub>2</sub> NiCd (SCN) <sub>4</sub>	40.52	40.34	2.19	2.43	13.5	13.73

## 4.2. Infrared spectra

According to the data presented in Table 4, the infrared spectra of the Schiff base ligands L<sub>1</sub> and L<sub>2</sub> exhibit absorption bands at 1658 cm<sup>-1</sup> and 1606 cm<sup>-1</sup>, respectively, which can be attributed to the C=N stretching vibration, as shown in Fig.3 and Fig.4. However, in the spectra of the corresponding complexes (Fig.5 - Fig.8), the C=N absorption band shifts to higher wavenumbers, indicating the coordination of the azomethine nitrogen to the metal ion. Additionally, absorption bands in the range of 2108-2148 cm<sup>-1</sup> are observed in the spectra of these complexes, which can be attributed to the formation of bridging thiocyanate groups [17].

**Table 4 . IR data of the ligand and its complexes**

Comp.	$\nu$ (C-H) Ar cm <sup>-1</sup>	$\nu$ (C-H) Alp cm <sup>-1</sup>	$\nu$ (C=N) cm <sup>-1</sup>	$\nu$ (C=C) cm <sup>-1</sup>	$\nu$ (C-N) in M- SCN-M cm <sup>-1</sup>	$\nu$ (M-N) cm <sup>-1</sup>
L <sub>1</sub>	3078 3022	2904	1658	1583	-	-
L <sub>1</sub> Co	3064	2945	1660	1593	2108 2090	557
L <sub>1</sub> Ni	3055	2947 2899	1672	1597	2086	646
L <sub>2</sub>	3197 3057	2889	1606	1529	-	-
L <sub>2</sub> Co	3057	2910	1631	1512	2146	-
L <sub>2</sub> Ni	3059	2948	1631	1508	2148	-

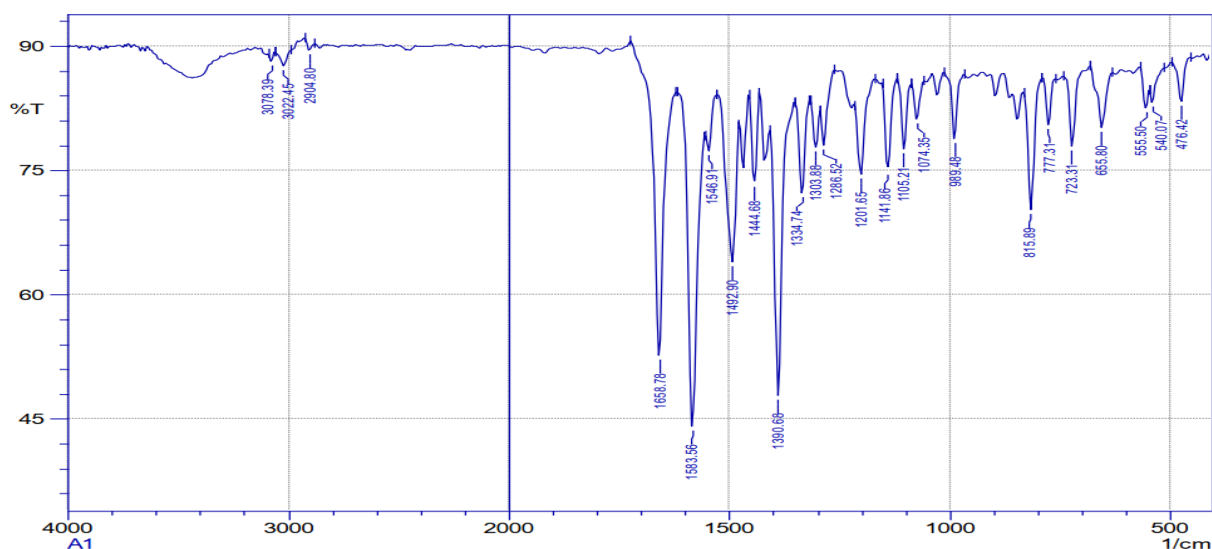


**Fig. 3.** Infrared Spectrum of ligand L<sub>1</sub>

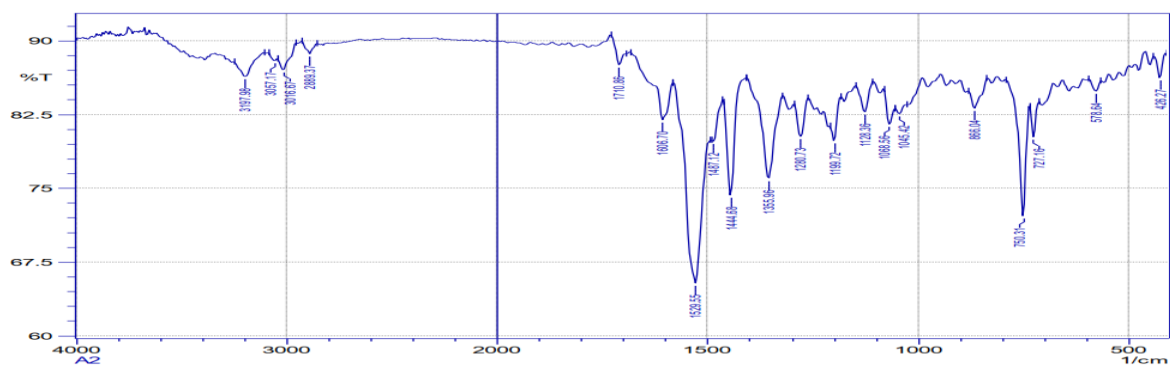


Fig. 4. Infrared Spectrum of ligand L<sub>2</sub>

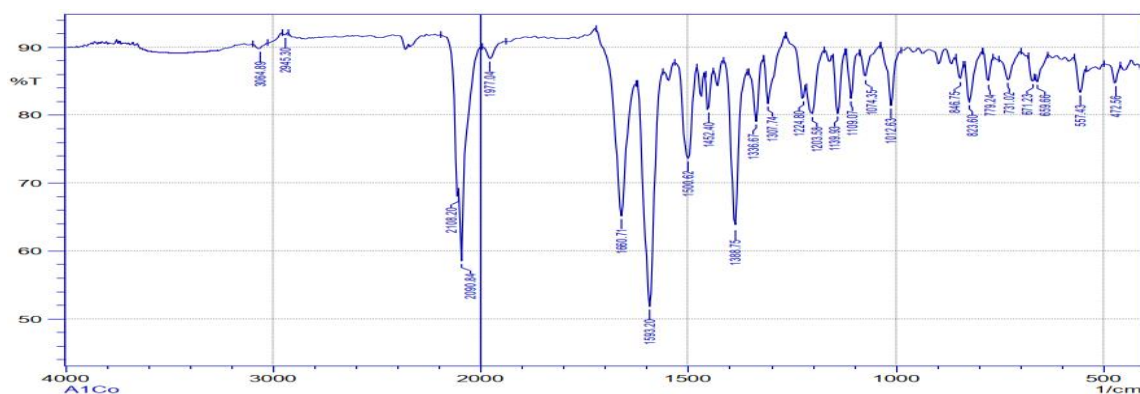


Fig. 5. Infrared Spectrum of complex L<sub>1</sub>Co

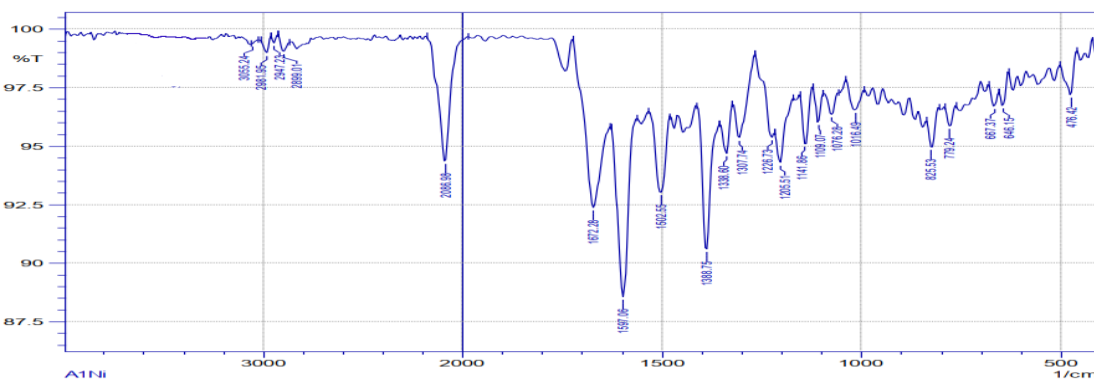


Fig. 6. Infrared Spectrum of complex L<sub>1</sub>Ni

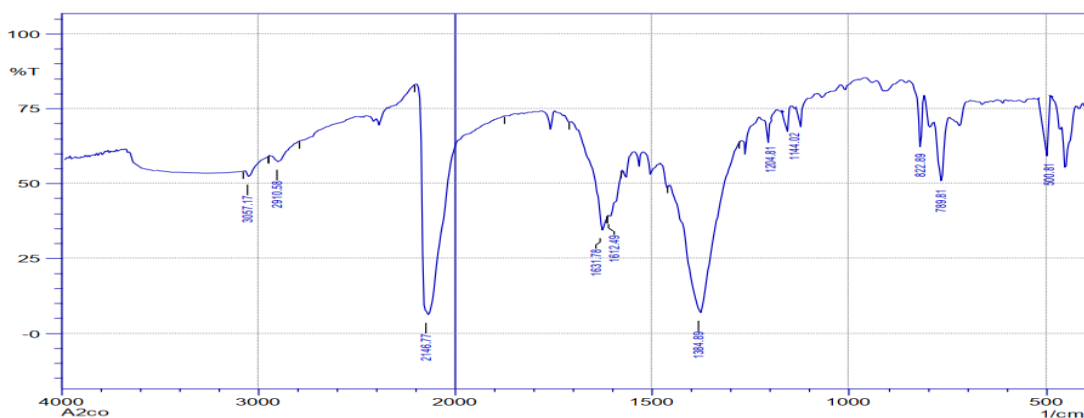


Fig. 7. Infrared Spectrum of complex L<sub>2</sub>Co



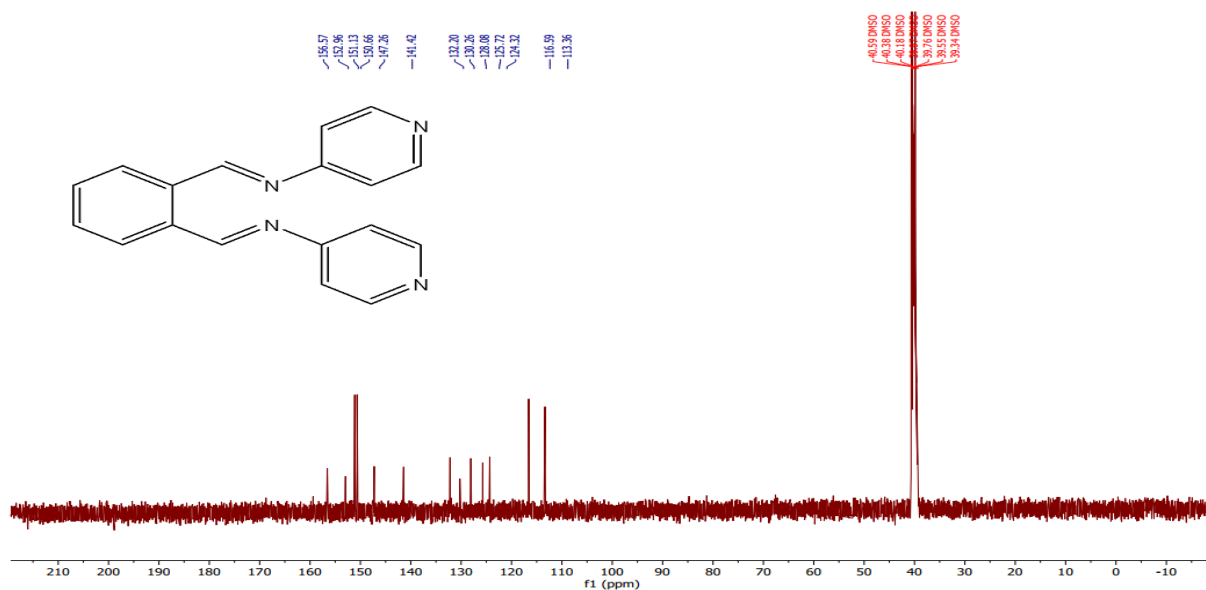


Fig. 11. <sup>13</sup>CNMR spectrum of ligand L<sub>1</sub>

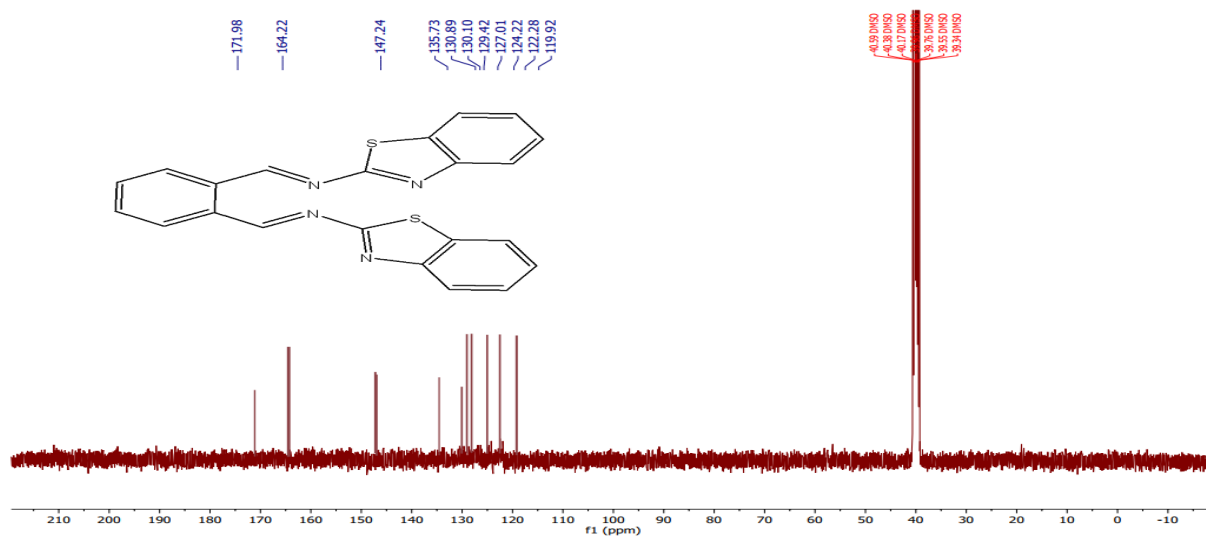


Fig. 12. <sup>13</sup>CNMR spectrum of ligand L<sub>2</sub>

#### 4.4. Mass spectra

Spectra of the mass exhibited clear signals for the molecular ion of the prepared compounds. Signals appeared at  $m/z = 285.1$  and  $398.2$ , corresponding to the molecular ions of L<sub>1</sub> and L<sub>2</sub>, respectively, as shown in Fig. 13 and Fig. 14. Furthermore, all complexes showed signals for both the molecular ion and the basic ion, as depicted in Fig. 15-18. This confirms the validity of the proposed structures for the compounds.

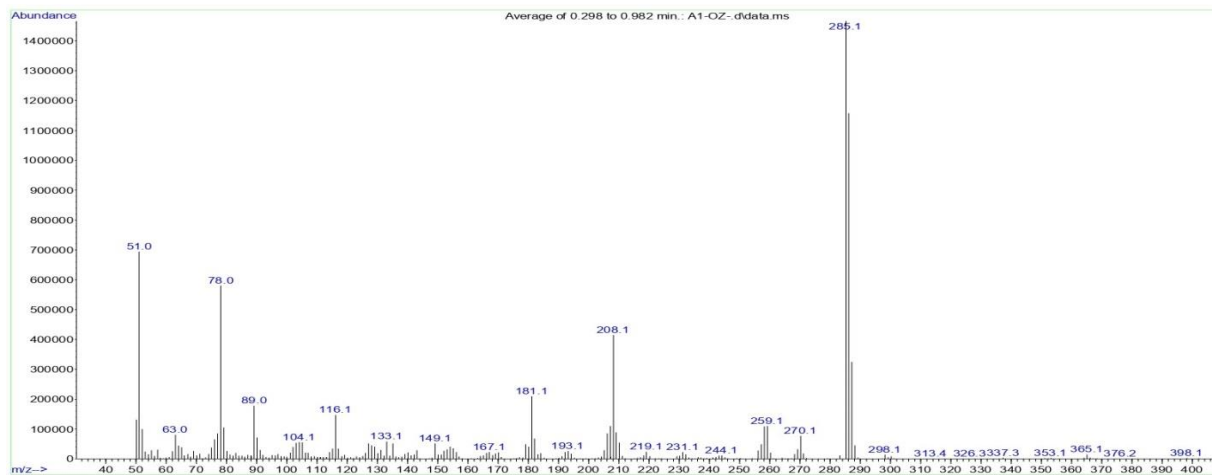


Fig. 13 . Mass spectrum of L<sub>1</sub>

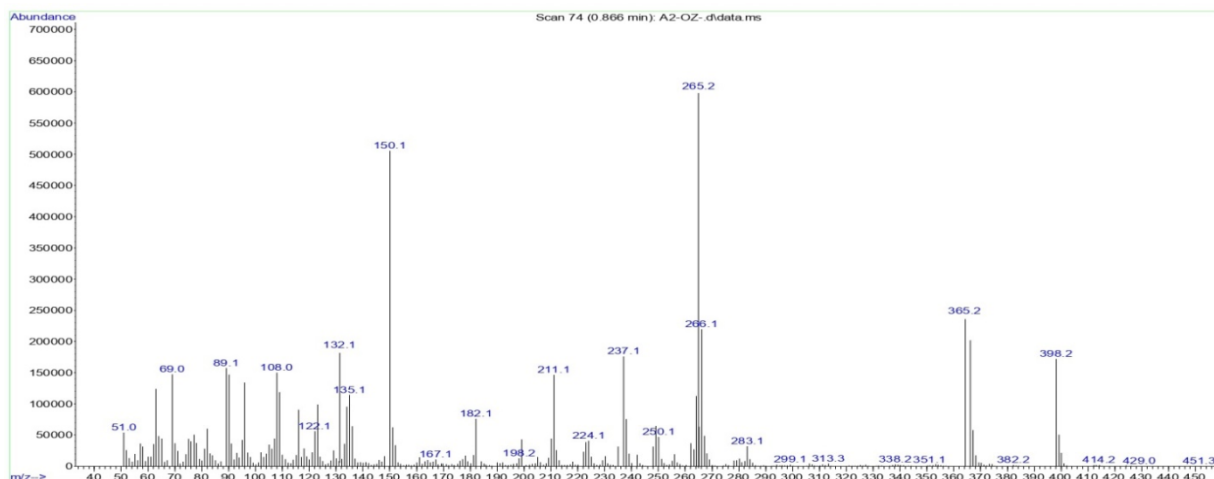


Fig. 14 . Mass spectrum of L<sub>2</sub>

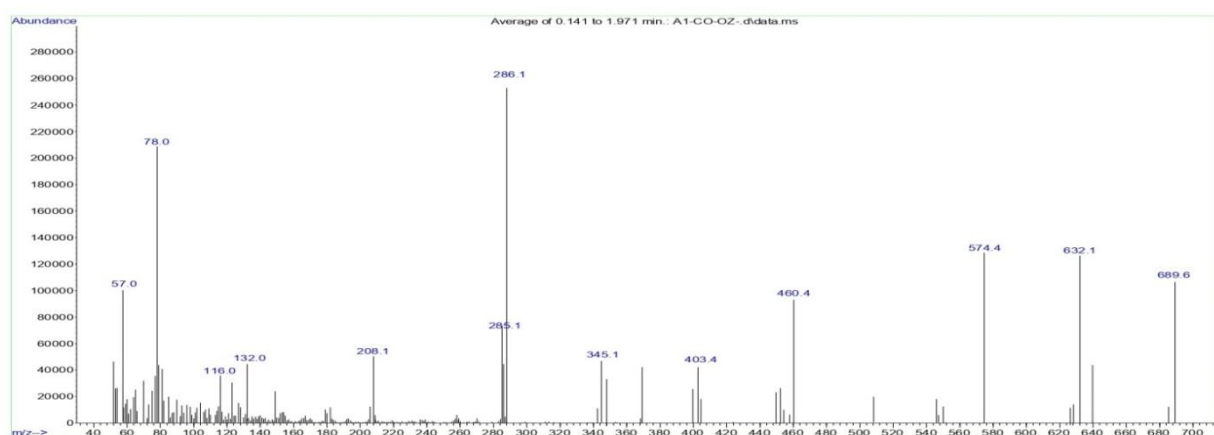


Fig. 15 . Mass spectrum of L<sub>1</sub>Co

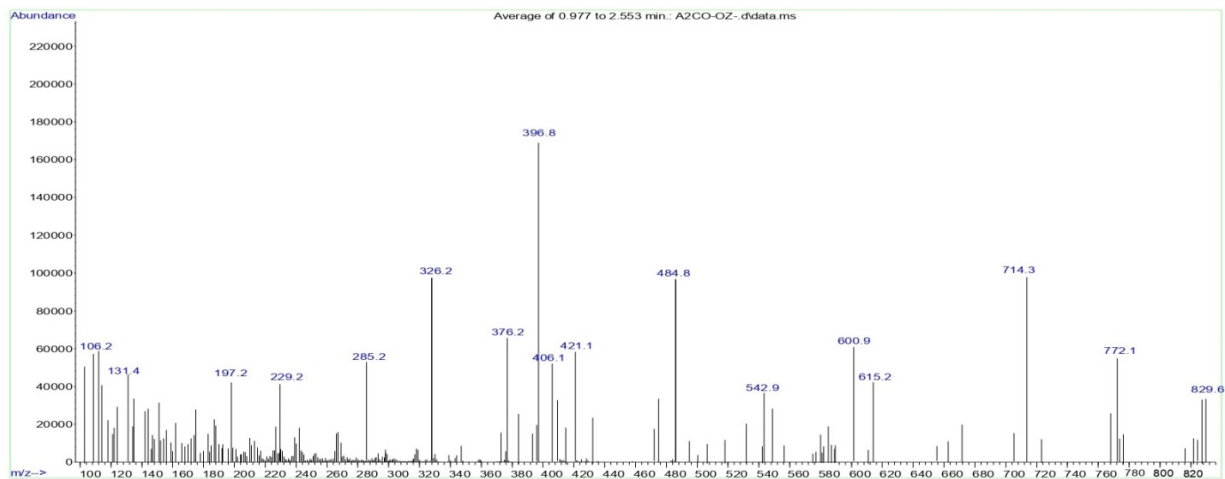


Fig. 16 . Mass spectrum of  $L_2Co$

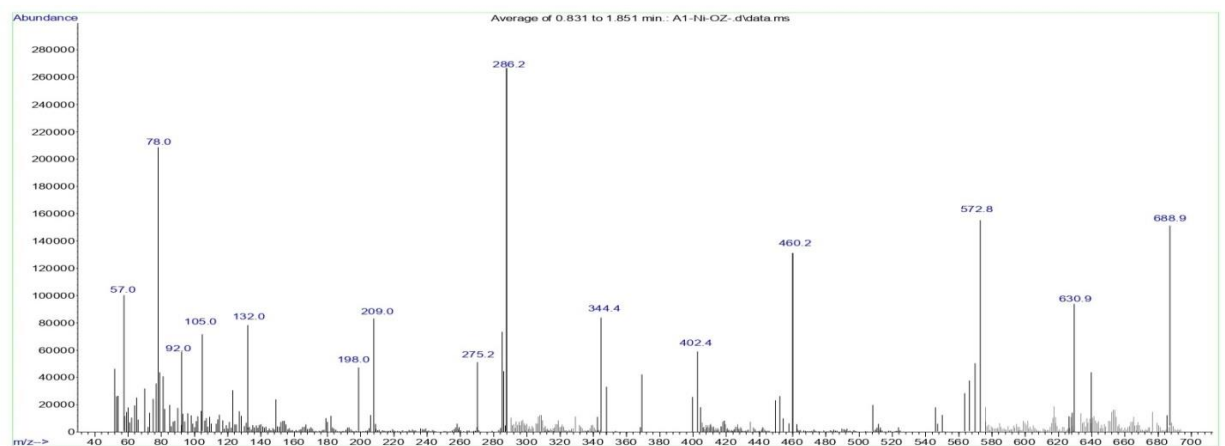


Fig. 17 . Mass spectrum of  $L_1Ni$

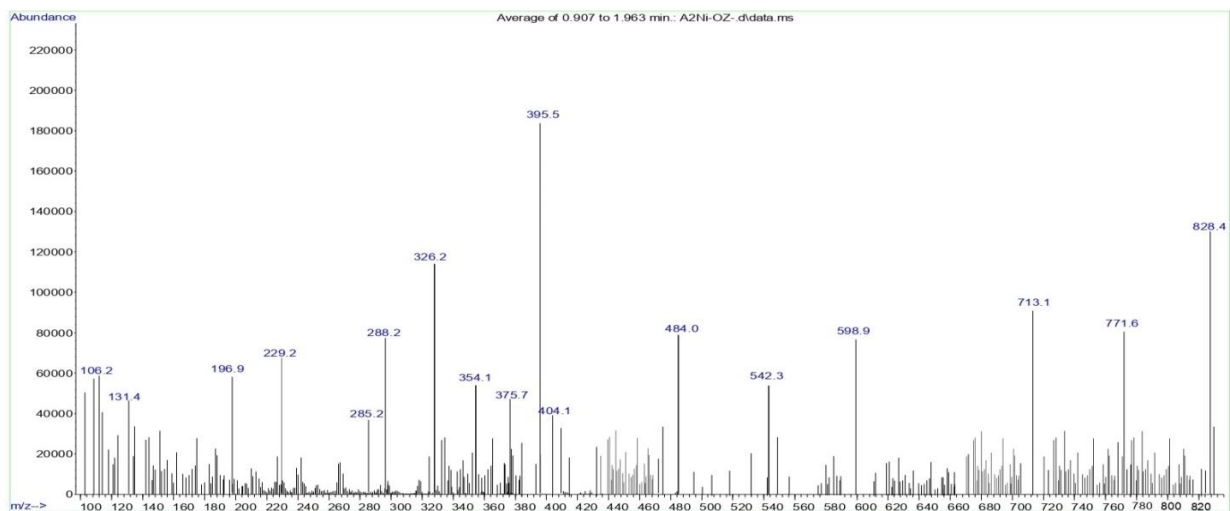


Fig. 18 . Mass spectrum of  $L_2Ni$

#### 4.5. Conductivity and magnetic susceptibility measurements

The molar conductivities of the synthesized complexes showed low values (17.6-18.5 S.cm<sup>2</sup>.mol<sup>-1</sup>), indicating the absence of negative ions outside the coordination sphere as shown in Table 5. The magnetic sensitivity results in Table 6 demonstrated that the cobalt complexes exhibited paramagnetic properties, with magnetic moments of (3.96,4.13 BM) for L<sub>1</sub>Co and L<sub>2</sub>Co, respectively, indicating their tetrahedral geometry with sp<sup>3</sup> hybridization. On the other hand, the low magnetic moments observed for the nickel complexes suggest diamagnetic properties, indicating a square planar geometry with dsp<sup>2</sup> hybridization [17].

**Table 5.** Molar conductivity measurements

Sym.of comp.	Chemical formula	Electrical conductivity ×10 <sup>-6</sup> Ohm <sup>-1</sup>	Molar conductivity (Ohm <sup>-1</sup> .cm <sup>2</sup> .mol <sup>-1</sup> )	Electrolytic Properties
L <sub>1</sub> Co	C <sub>18</sub> H <sub>14</sub> N <sub>4</sub> CoCd (SCN) <sub>4</sub>	16.2	17.8	Non electrolyte
L <sub>2</sub> Co	C <sub>22</sub> H <sub>14</sub> N <sub>4</sub> S <sub>2</sub> CoCd (SCN) <sub>4</sub>	16	17.6	Non electrolyte
L <sub>1</sub> Ni	C <sub>18</sub> H <sub>14</sub> N <sub>4</sub> NiCd (SCN) <sub>4</sub>	16.9	18.5	Non electrolyte
L <sub>2</sub> Ni	C <sub>22</sub> H <sub>14</sub> N <sub>4</sub> S <sub>2</sub> NiCd (SCN) <sub>4</sub>	16.1	17.7	Non electrolyte

**Table 6.** Magnetic susceptibility measurements

Sym.	Chemical formula	- D ×10 <sup>-6</sup>	X <sub>g</sub> ×10 <sup>-6</sup>	X <sub>M</sub> ×10 <sup>-3</sup>	X <sub>A</sub> ×10 <sup>-3</sup>	μ <sub>eff</sub> B.M.	Hyb.	Geometry	Magnetic Properties
L <sub>1</sub> Co	C <sub>18</sub> H <sub>14</sub> N <sub>4</sub> CoCd (SCN) <sub>4</sub>	380.3	9.01	6.21	6.59	3.96	Sp <sup>3</sup>	Tetrahedral	Paramagnetic
L <sub>2</sub> Co	C <sub>22</sub> H <sub>14</sub> N <sub>4</sub> S <sub>2</sub> CoCd (SCN) <sub>4</sub>	440.8	8.10	6.73	7.17	4.13	Sp <sup>3</sup>	Tetrahedral	Paramagnetic
L <sub>1</sub> Ni	C <sub>18</sub> H <sub>14</sub> N <sub>4</sub> NiCd (SCN) <sub>4</sub>	380.3	0	0	380.3	0.95	dsp <sup>2</sup>	Square planar	Diamagnetic
L <sub>2</sub> Ni	C <sub>22</sub> H <sub>14</sub> N <sub>4</sub> S <sub>2</sub> NiCd (SCN) <sub>4</sub>	440.8	0	0	440.8	1.02	dsp <sup>2</sup>	Square planar	Diamagnetic

#### 5. Corrosion study

Polarization curves were investigated in an acidic medium with a 1 M concentration of hydrochloric acid solution for N80 carbon steel alloy in the presence and absence of inhibitors. These measurements were conducted within the range of ±400 millivolts. From figures 19 and 20 for compounds L1 and L2 at 298 Kelvin, it is observed that an increase in the concentration of the inhibitor leads to a slight alteration in the corrosion potential values (E<sub>corr</sub>). If the difference between the corrosion potential value (E<sub>corr</sub>) in the presence of the inhibitor and the corrosion potential value (E<sub>corr</sub>) in the absence of the inhibitor exceeds 80 millivolts, it indicates that the inhibitor is either cathodic or anodic. However, if the difference is less than 50 millivolts, it suggests that the inhibitors are of the mixed-type. The addition of the inhibitor to the acidic solution hinders the anodic reaction and delays the release of hydrogen gas during the cathodic reaction [19].

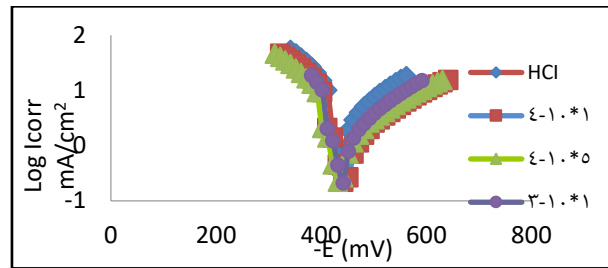


**Fig. 19.** Polarization curve (Tafel plot) of L<sub>1</sub>

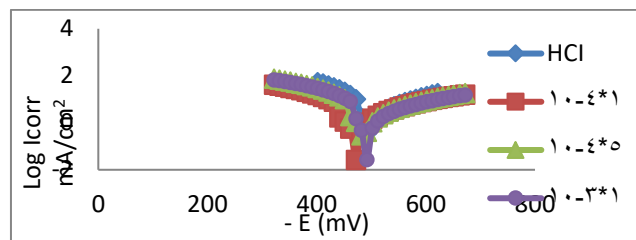


**Fig. 20.** Polarization curve (Tafel plot) of L<sub>2</sub>

The percentage efficiency of inhibition (IE%) and the fraction covered by inhibition ( $\Theta$ ) were calculated using the following equations:

$$\% \text{ IE} = ((I^{\circ}\text{corr} - I_{\text{corr}}) / I^{\circ}\text{corr}) \times 100$$

$$\Theta = (I^{\circ}\text{corr} - I_{\text{corr}}) / I_{\text{corr}}$$

Here,  $I^{\circ}\text{corr}$  and  $I_{\text{corr}}$  represent the corrosion current density in the absence and presence of the inhibitor, respectively. It was observed that the corrosion current density values in the blank solution, without the inhibitors, were higher than the values in the presence of inhibitors. Additionally, the corrosion current density decreased with increasing inhibitor concentrations at each temperature, indicating that the addition of the inhibitor slows down the corrosion rate.

The corrosion rate (CR) of N80 carbon steel alloy in the acidic medium was also calculated in the absence and presence of different concentrations of the used scale inhibitors at temperatures of 298K, 308K, and 318K, using the following equation:

$$\text{CR} = K \times (I_{\text{corr}} / \rho \times \text{EW})$$

Here, CR represents the corrosion rate in units of mpy (thousandths of an inch per year),  $I_{\text{corr}}$  represents the corrosion current density in units of  $\mu\text{A}/\text{cm}^2$ , EW represents the equivalent weight in units of gm/mol,  $\rho$  represents the density of the metal or alloy in units of  $\text{g}/\text{cm}^3$ , and K is a constant value equal to 0.1288 mpy g /  $\mu\text{A cm}$ .

From the obtained results in Table 7 it is evident that the corrosion rate (CR) shows a relative increase in the absence of inhibitors, indicating that the metal dissolution reaction is responsible for this increase. On the other hand, the presence of inhibitors reduces the corrosion rate of the N80 carbon steel alloy, resulting in a decrease in the corrosion current on the alloy surface.

The effect of temperature and concentration on the inhibition efficiency was studied, as shown in Fig. 21 and Fig.22. The inhibition efficiency values were found to increase proportionately with increasing temperature while maintaining the same concentration. While the temperature remains constant, they also increase with increasing inhibitor concentration, as shown in Figure 23 and Figure 24 . This can be attributed to the chemical absorption of the inhibitor on the carbon steel surface, which is favored by high temperatures. Notably, the inhibition rate decreases with increasing temperature in the physical drying process. Based on these findings, we can conclude that the observed inhibition is due to the chemical absorbers [20,21].

**Table 7.** Data on the polarization curves of the corrosion of carbon steel N80 at different concentrations of L<sub>1</sub> and L<sub>2</sub> inhibitors at different temperatures

Comp.	$\theta$	%IE	$\beta_c$ mv/Dec	$\beta_a$ mV/Dec	$I_{corr}$ mA/cm <sup>2</sup>	CR mpy	-E <sub>corr</sub> mV	Inhibitor Conc. M	Temp. K
HCl	0	0	66.2	-174.1	13.35	6.08	443.2		298
	0	0	86.5	-188.9	18.83	8.57	477.3	Blank	308
	0	0	79.0	-172.4	28.41	12.94	474.7		318
L <sub>1</sub>	0.84	84.04	80.9	-155.5	2.13	0.97	475		298
	0.86	86.77	94	-220	2.49	1.13	473	1*10 <sup>-4</sup>	308
	0.90	90.35	94.2	-183.6	2.74	1.24	473.1		318
	0.85	85.16	57.9	-123.1	1.98	0.90	455.5		298
	0.88	88.68	74.9	-143.8	2.13	0.97	442.1	5*10 <sup>-4</sup>	308
	0.91	91.27	79.1	-141.6	2.48	1.129	437.2		318
	0.85	85.99	56.1	-103.0	1.87	0.85	411.2		298
	0.89	89.64	59.9	-129.2	1.95	0.88	401.8	1*10 <sup>-3</sup>	308
	0.92	92.32	60.0	-114	2.18	0.99	403		318
L <sub>2</sub>	0.75	75.43	109.5	-146.2	3.28	1.49	473.5		298
	0.82	82.04	96	-144	3.38	1.53	473.7	1*10 <sup>-4</sup>	308
	0.86	86.30	95.4	-150.9	3.89	1.77	466.3		318
	0.76	76.77	57.9	-126.8	3.1	1.41	483		298
	0.82	82.47	55.3	-124.4	3.3	1.50	475.4	5*10 <sup>-4</sup>	308
	0.87	87.71	73.2	-111.3	3.49	1.58	480.1		318
	0.79	79.32	64.7	-94.1	2.76	1.25	492.6		298
	0.84	84.17	82.8	-111.5	2.98	1.35	482.7	1*10 <sup>-3</sup>	308
0.88	88.27	68.6	-123.4	3.33	1.51	472.2		318	

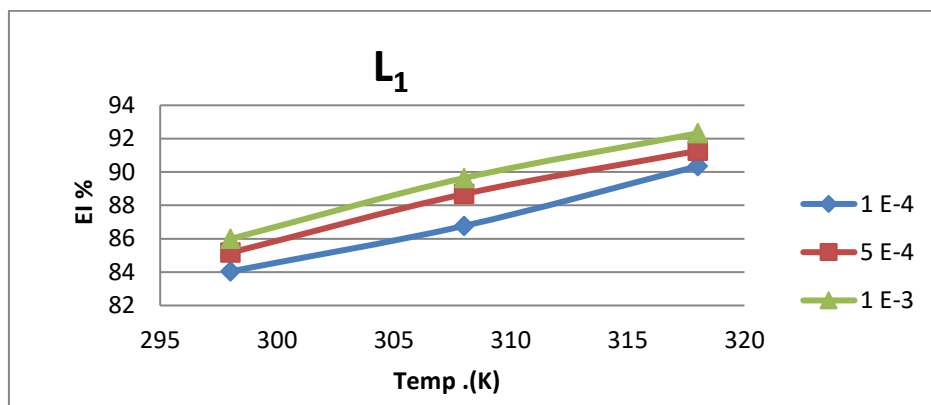


Fig. 21. (IE%) and temperature at different concentrations of inhibitor L<sub>1</sub>

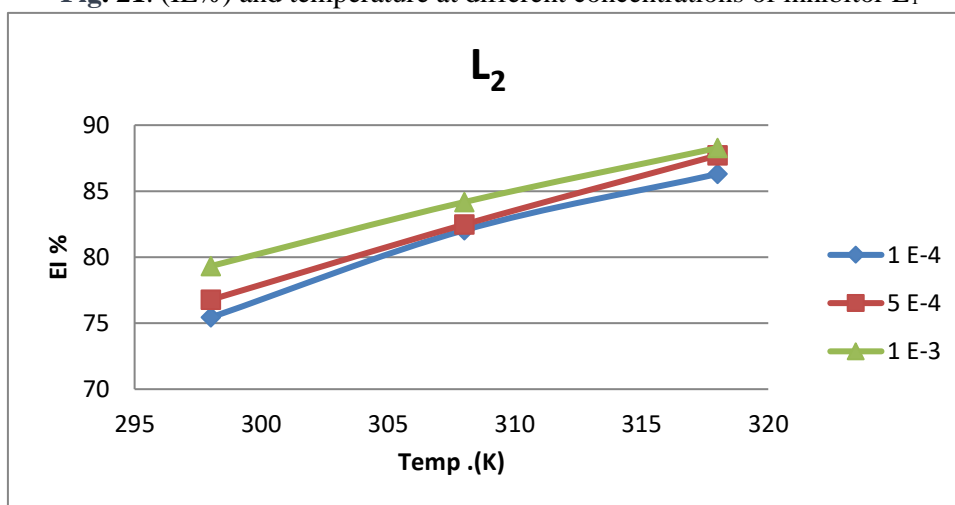


Fig. 22. (IE%) and temperature at different concentrations of inhibitor L<sub>2</sub>

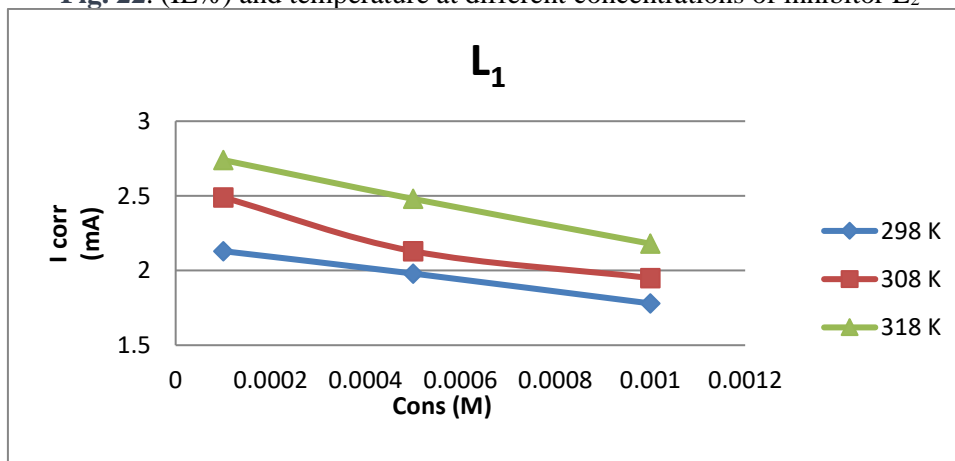


Fig. 23. Effect of concentration variation on L<sub>1</sub> corrosion

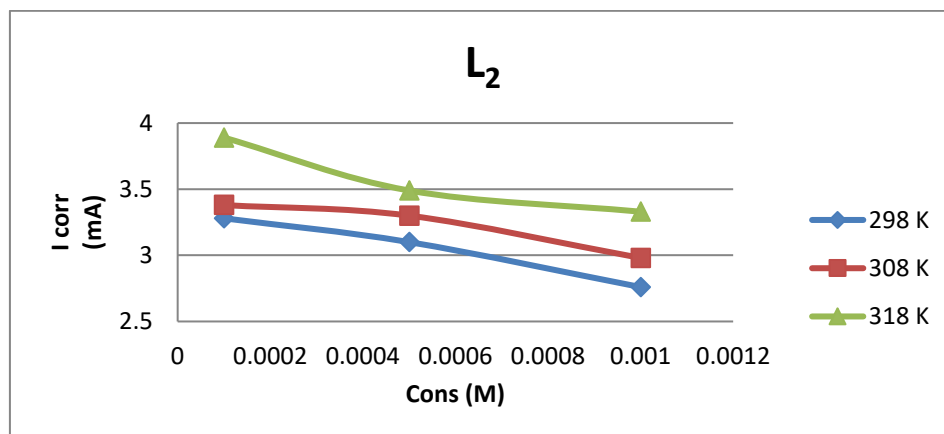


Fig. 24. Effect of concentration change on the corrosion current of L<sub>2</sub>

## 6. Conclusion

The results of this study showed that the synthesized compounds L<sub>1</sub> and L<sub>2</sub> are organic corrosion inhibitors, as they are attracted to the surface of the N80 carbon-steel alloy, and this is confirmed by electrochemical polarization (Tafel curves) at different temperatures, I<sub>corr</sub>, E<sub>corr</sub>, and IE %. It was also observed that compound L<sub>1</sub> is more effective as an inhibitor compared to compound L<sub>2</sub>, as evidenced by the obtained results in this study, where the highest inhibition efficiency reached 92.32% at a temperature of 318 K and a concentration of 1\*10<sup>-3</sup> M

## 7. References

- [1] H. Schiff, "Mittheilungen aus dem Universitätslaboratorium in Pisa: Eine neue Reihe organischer Basen," *Justus Liebigs Annalen Der Chemie*, vol. 131, no. 1, pp. 118–119, Jan. 1864, doi: <https://doi.org/10.1002/jlac.18641310113>
- [2] E. Amenu, "Use and management of medicinal plants by indigenous people of Ejaji area (Chelya Woreda) West Shoa, Ethiopia: An ethnobotanical approach." In *M. Sc. Thesis* (2007). doi:<https://shorturl.at/bxBLX>
- [3] A. Zopiatis, "Is it art or science? Chef's competencies for success," *International Journal of Hospitality Management*, vol. 29, no. 3, pp. 459–467, Sep. 2010, doi: <https://doi.org/10.1016/j.ijhm.2009.12.003>
- [4] J. Liang, Q. Han, Y. Tan, H. Ding, and J. Li, "Current advances on Structure-Function relationships of pyridoxal 5'-Phosphate-Dependent enzymes," *Frontiers in Molecular Biosciences*, vol. 6, Mar. 2019, Doi: <https://doi.org/10.3389/fmolb.2019.00004>
- [5] T. A. Martin and W. G. Jiang, "Editorial [Hot topic: Hepatocyte Growth Factor and cMET, New Development in Cancer Therapies (Guest Editors: T.A. Martin and W.G. Jiang)]," *Anti-cancer Agents in Medicinal Chemistry*, vol. 10, no. 1, p. 1, Jan. 2010, Doi: <https://doi.org/10.2174/1871520611009010001>
- [6] N. S. Gwaram, "Synthesis and characterization of a Schiff base Cobalt (III) complex and assessment of its anti-cancer activity," *Chemsearch Journal*, vol. 8, p.56, 2017.
- [7] S. H. Kadhim, I. Q. Abd-Alla and T. J. Hashim, "Synthesis and Characteristic Study of Co (II), Ni (II) And Cu (II) Complexes of New Schiff Base Derived from 4-Amino Antipyrine," *Int J Chem Sci*, vol. 15, p. 107, 2017.
- [8] S. Satpati, A. Suhasaria, S. Ghosal, S. Dey, and D. Sukul, "Interaction of newly synthesized dipeptide Schiff bases with mild steel surface in aqueous HCl: Experimental and theoretical study on thermodynamics, adsorption and anti-corrosion characteristics," *Materials Chemistry*

- and Physics*, vol. 296, p. 127200, Feb. 2023, doi: <https://doi.org/10.1016/j.matchemphys.2022.127200>
- [9] H. Jafari, E. Ameri, M. Rezaeivala, A. Berisha, and J. Halili, "Anti-corrosion behavior of two N<sub>2</sub>O<sub>4</sub> Schiff-base ligands: Experimental and theoretical studies," *Journal of Physics and Chemistry of Solids*, vol. 164, p. 110645, May 2022, Doi: <https://doi.org/10.1016/j.jpics.2022.110645>
- [10] C. U. Ibeji, D. C. Akintayo, H. O. Oluwasola, E. O. Akintemi, O. G. Onwukwe, and O. M. Eziomume, "Synthesis, experimental and computational studies on the anti-corrosion performance of substituted Schiff bases of 2-methoxybenzaldehyde for mild steel in HCl medium," *Scientific Reports*, vol. 13, no. 1, Feb. 2023, Doi: <https://doi.org/10.1038/s41598-023-30396-3>
- [11] A. Khezri, L. Edjlali, M. Es'haghi, M. T. Vardini, and H. Basharnavaz, "Addition of Schiff bases to hybrid Silane Sol–Gel coatings: An efficient strategy to develop an active system for corrosion protection of copper," *Journal of Materials Engineering and Performance*, vol. 32, no. 23, pp. 10740–10749, Feb. 2023, Doi: <https://doi.org/10.1007/s11665-023-07878-6>
- [12] S. Kumar and V. K. Swami, "A COMPARATIVE STUDY OF INHIBITIVE EFFECTS OF SOME NEW SCHIFF BASES ON COPPER CORROSION IN ACIDIC MEDIUM," *Journal of Advanced Scientific Research*, vol. 13, no. 02, pp. 176–182, Mar. 2022, doi: <https://doi.org/10.55218/JASR.202213223>
- [13] U. Nazir, Z. Akhter, N. Z. Ali, R. Hussain, F. Liaqat, A. Tahir and S. Qamar, "Corrosion inhibition studies of ferrocenyl Schiff bases in a mild acidic medium through experimental methods and DFT calculations," *New Journal of Chemistry*, vol. 46, no. 8, pp. 3925–3938, Jan. 2022, Doi: <https://doi.org/10.1039/D1NJ05612C>
- [14] U. Nazir, Z. Akhter, N. K. Janjua, M. A. Asghar, S. Kanwal, T. M. Butt and F. U. Shah, "Biferrocenyl Schiff bases as efficient corrosion inhibitors for an aluminium alloy in HCl solution: a combined experimental and theoretical study," *RSC Advances*, vol. 10, no. 13, pp. 7585–7599, Jan. 2020, Doi: <https://doi.org/10.1039/C9RA10692H>
- [15] O. A. El-Gammal, F. Sh. Mohamed, G. N. Rezk, and A. A. El-Bindary, "Structural characterization and biological activity of a new metal complexes based of Schiff base," *Journal of Molecular Liquids*, vol. 330, p. 115522, May 2021, Doi: <https://doi.org/10.1016/j.molliq.2021.115522>
- [16] A. H. Jasim, M. Y. Kadhum, and S. Q. Badr, "Spectral Properties and Biological Activities of Binuclear Mixed-Metal Bridged Thiocyanate Complexes Containing Schiff Bases Derived from Isatin," *Engineering Proceedings*, vol. 59, p. 237, 2024, Doi: <https://doi.org/10.3390/engproc2023059237>
- [17] M. Y. Kadhum and B. J. Al-musawi, "Preparation, identification and antimicrobial studies of some bimetallic bridged thiocyanates complexes containing N, N'-bis (4-isopropyl benzylidene) 4-methyl benzene-1, 2-diamine Schiff base ligand." *Adv. Appl. Sci. Res*, vol. 6, p. 120-129, 2015.
- [18] N. Berber, "Synthesis of new Schiff base compounds and identification of their structures," *Adiyaman ÜNiversitesi Fen Bilimleri Dergisi*, Jun. 2020, Doi <https://doi.org/10.37094/adyujsci.633080>
- [19] A. Sehmi, H. B. Ouici, A. Guendouzi, M. Ferhat, O. Benali, and F. Boudjellal, "Corrosion Inhibition of Mild Steel by newly Synthesized Pyrazole Carboxamide Derivatives in HCl Acid Medium: Experimental and Theoretical Studies," *Journal of the Electrochemical Society*, vol. 167, no. 15, p. 155508, Jan. 2020, Doi: <https://doi.org/10.1149/1945-7111/abab25>

- [20] Y. Elkhofri, I. Forsal, E. M. Rakib, and B. Mernari, "The inhibition action of essential oil of *J. juniperus phoenicea* on the corrosion of mild steel in acidic media," *Portugaliae Electrochimica Acta*, vol. 36, no. 2, pp. 77–87, Jan. 2018, doi: <https://doi.org/10.4152/pea.201802077>
- [21] G. Palumbo, M. Górny, and J. Banaś, "Corrosion Inhibition of pipeline carbon steel (N80) in CO<sub>2</sub>-Saturated chloride (0.5 m of KCL) solution using gum arabic as a possible environmentally friendly corrosion inhibitor for shale gas industry," *Journal of Materials Engineering and Performance*, vol. 28, no. 10, pp. 6458–6470, Oct. 2019, Doi: <https://doi.org/10.1007/s11665-019-04379-3>

## تحضير وتشخيص بعض قواعد شف المشتقة من الاورثوفتالديهايد ومعقداتها الجسرية مع $Ni(II)$ و $Co(II)$ كمثبطات لتاكل الفولاذ الكربوني في الوسط الحامضي

اثير ناجي ابو الهيل ، مؤيد يوسف كاظم

قسم الكيمياء ، كلية التربية للعلوم الصرفة ، جامعة البصرة ، البصرة ، العراق

### الملخص

### معلومات البحث

في هذه الدراسة تم تحضير ليكاندين لقواعد شف  $L_1$  و  $L_2$  مشتقة من الاورثوفتالديهايد مع امينين اولية هما 4-امينو بريدين و 4-امينو بنزو ثايذول وشخصت بواسطة مطيافية الاشعة تحت الحمراء والرنين النووي المغناطيسي للبروتون ونظير الكربون 13 ومطيافية الكتلة وتحليل العناصر . بعد ذلك تم مفاعلة الليكاندات المحضرة مع التتراثايوسيانات بنسبة مولية 1:1 لينتج معقدات جسرية من نوع  $LMCd(SCN)_4$  حيث ان M تمثل  $Co(II)$  او  $Ni(II)$  وقد شخصت تلك المعقدات ايضا بعدة طرق طيفية و قياسات الحساسية المغناطيسية. لقد بينت النتائج بان كل المعقدات المحضرة ذات عدد تناسقي يساوي اربعة وان معقدات الكوبلت تمتلك خواص بارامغناطيسية وان معقدات النيكل تكون ديامغناطيسية . بالاضافة الى ذلك تم تقييم كفاءة ليكاندات قواعد شف المحضرة كمثبطات لتاكل الفولاذ الكربوني في الوسط الحامضي وق د اظهرت كفاءة تثبيطية جيدة

الاستلام 10 نيسان 2024  
القبول 30 ايار 2024  
النشر 30 حزيران 2024

### الكلمات المفتاحية

قاعدة شف ، اورثوفتالديهايد ، مثبطات ، تاكل

**Citation:** Atheer N. A., Mouayed Y. K., J. Basrah Res. (Sci.) 50(1), 251 (2024).  
DOI:<https://doi.org/10.56714/bjrs.50.1.20>

\*Corresponding author email : atheer.naji@uobasrah.edu.iq



©2022 College of Education for Pure Science, University of Basrah. This is an Open Access Article Under the CC by License the [CC BY 4.0](https://creativecommons.org/licenses/by/4.0/) license.

ISSN: 1817-2695 (Print); 2411-524X (Online)  
line at: <https://jou.jobrs.edu.iq>